DOI: 10.19884/j.1672-5220.202311003

Hardware-in-the-Loop Simulation System Based on Unity3D for Winding Machine

TANG Long, ZOU Kun*
College of Mechanical Engineering, Donghua University, Shanghai 201620, China

Abstract: Research and development of mechatronic products generally face the problems of large workload, long cycle and high cost of on-site debugging, and the current mainstream simulation software has a single function. Thus, a set of hardware-in-the-loop simulation (HILS) system with both real time and a three-dimensional (3D) display effect is designed, and can be connected to the mechatronic software. The winding machine is taken as the simulation object, a virtual simulation platform using Unity3D is built, and the real-time interaction of data between the virtual simulation platform and the control system is realized through the circuit board. The feasibility of the process simulation of the electromechanical system in the winding machine is verified by outputting the motion timing and spatial trajectory diagrams of the key structures in the winding process. The results show that the system can replace part of the on-site debugging work and improve the efficiency of research and development.

Key words: hardware-in-the-loop simulation (HILS); winding machine; real time; Unity3D; three-dimensional (3D) display; simulation circuit board; process simulation
CLC number: TP391.9 **Document code**: A
Article ID: 1672-5220(2024)03-0298-10

Open Science Identity (OSID)

0 Introduction

Hardware-in-the-loop simulation (HILS) refers to a simulation technology that introduces part of the physical products into the simulation loop[1], and usually consists of physical components, a signal conditioning unit, an emulation computer and an upper computer, as shown in Fig. 1. The digital models run on the emulation computer in the form of software, the emulation computer communicates with the physical components through a signal conditioning unit, and the upper computer is used to manage the operation of the emulation computer.

Early HILS was mainly applied in the field of defense and aerospace. With the development of computer control technology and its integration into electromechanical systems[2], the application of HILS is more and more extensive. In the automotive field, Chung et al.[3] applied dynamic path planning and model predictive control techniques to simulate the parking and autonomous driving of an electric truck, and verified the feasibility of shifting from manual to autonomous driving, dynamic route planning, obstacle avoidance and automatic parking through HILS. In the field of robotics, Sahoo et al.[4] designed and developed HILS for an omnidirectional mobile robot, and the control inputs of the simulation model were transmitted to the robot hardware through an Arduino microcontroller input board, which verified the validity of the method in the robot planarity control system. In the field of unmanned aircraft, Omar[5] developed HILS for a quadrotor suspended load system using Gazebo, and based on the dynamics of the system, an anti-swing controller was designed, which achieved good results. In the field of mechanical engineering, Kim et al.[6] proposed a method for evaluating the performance of machine tool feed drive position control and assessing the accuracy of the proposed method through HILS. In addition, nowadays HILS is widely used in other fields[7-20], such as engines and electronic power. At present, the commonly used HILS is more or less deficient, such as the dSPACE system and mathematical modeling with Simulink, although there is a strong real-time effect, but also lacks a better three-dimensional (3D) effect, and the cost is very expensive.

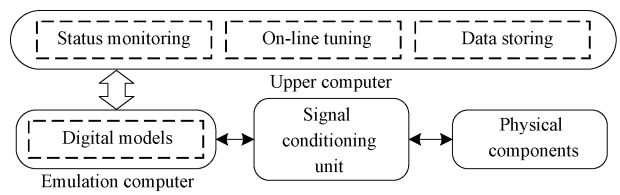

Fig. 1 HILS system composition

In order to realize the function of the simulation system, the selected virtual platform not only needs good 3D display, but also must ensure sufficient real-time effect, and can connect to the external hardware system for hardware and software debugging work. Therefore, this paper chooses Unity3D, a virtual reality engine[21], to build the platform.

Received date: 2023-11-03
Foundation item: National Key Research and Development Program of China (No. 2017YFB1304000)
* Correspondence should be addressed to ZOU Kun, email: kouz@dhu.edu.cn
Citation: TANG L, ZUN K. Hardware-in-the-loop simulation system based on Unity3D for winding machine[J]. *Journal of Donghua University (English Edition)*, 2024, 41(3): 298-307.

In addition, for the development and design of the winding machine, most manufacturers believe that the main problem is the gap between the mechanical structure and manufacturing precision of domestic and foreign winding machines. In fact, most of the manufacturers have purchased and assembled the foreign winding machine, and the results of the winding are still unsatisfactory, which means that there are obvious differences in the control program of the winding. Thus, it is especially important to design and develop a set of the HILS system to verify the control program of the winding machine nowadays.

This paper proposes the method of using Unity3D to connect the hardware electronic system to debug the control program, taking the winding machine as the research object, and designing a set of the HILS system. For the winding process, programmable logic controller (PLC) signals are used as the driver and the winding machine in Unity3D is used as the executing part to simulate the real winding situation and study the real time and accuracy of the simulation system. The research results would be of great significance in solving the problems of textile machinery development and debugging, and process design verification.

1 Simulation System Design

1.1 Overall scheme

The overall scheme of the simulation system is shown in Fig. 2. It consists of two subsystems, which are the virtual simulation platform and the real hardware control system. The real hardware control system includes the circuit board, PLC and the user host.

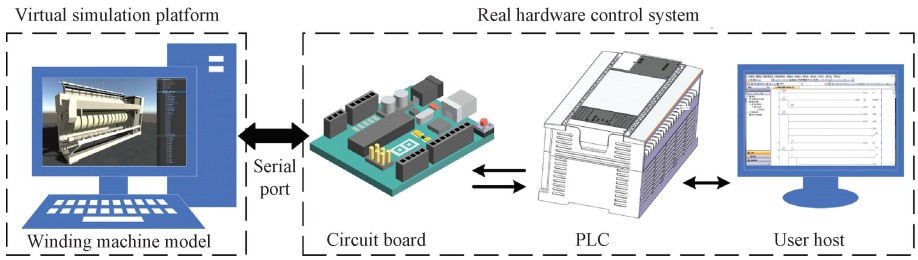

Fig. 2 Overall scheme of simulation system

The virtual simulation platform is built through Unity3D, and the serial port is used to receive PLC signals collected by the circuit board, and control the winding machine model in the virtual simulation platform in real time. At the same time, the virtual sensor signals generated during the movement of the winding machine (signals from the ray detection function triggered by the Unity3D physics engine) can be fed back to PLC through the circuit board. The whole simulation process can be monitored and controlled by the user host.

1.2 Construction of virtual simulation platform

Environment configuration and script design are two key parts of the virtual simulation platform construction, as shown in Fig. 3. The environment configuration includes scene setting and model import. Since Unity3D only supports FBX and OBJ formats, the model needs to be converted into a supportable file using 3dsMax (or modeling directly in 3dsMax), and then the simulation process can be clearly demonstrated in multiple directions by setting the light source parameters and the camera position in Unity3D, as shown in Fig. 4.

However, when the model is imported into Unity3D, because the Unity3D model only has a parent-child relationship, the model will lose the original mechanical fit, so the geometric constraint relationship of the key mechanism must be restored. To this end, two methods are designed: using 3dsMax to reselect the parent-child relationship; expanding the inspector panel parameters of Unity3D and selecting the target parts for constraint fit. As shown in Fig. 5, the expanded inspector panel parameters can be set according to the specific mechanical constraint relationship.

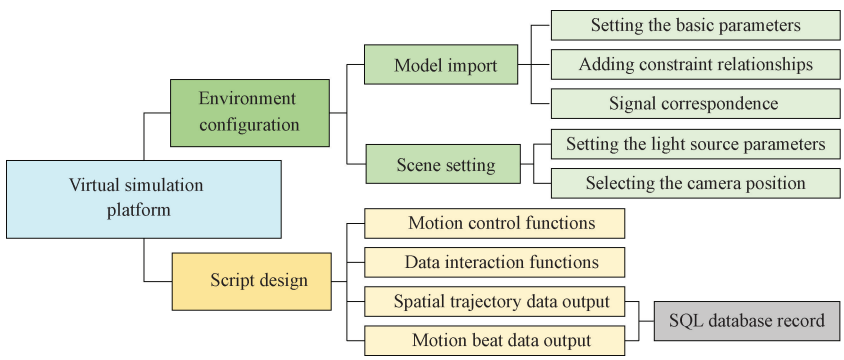

SQL——structured query language.

Fig. 3 Construction of virtual simulation platform

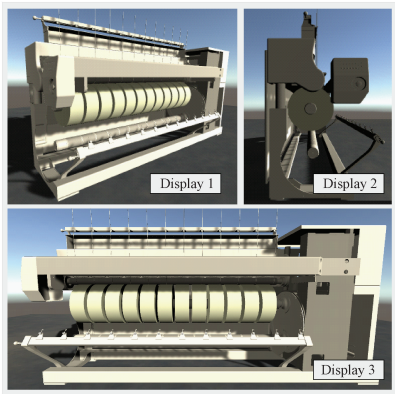

Fig. 4 Scene views in Unity3D

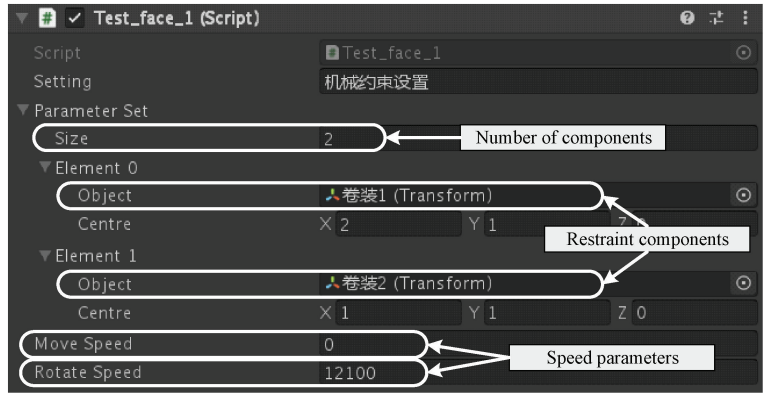

Fig. 5 Inspector panel

In order to realize the various functions of the virtual simulation platform, script design is required. Unity3D supports script editing in C#, and by writing specific function codes, the motion control functions and data interaction functions of the platform can be easily realized. Combined with the SQL database, Unity3D can also realize the output of spatial trajectory and motion beat data.

When the hardware control system runs the actual program, the real control signals are collected through the data interaction functions to control the real-time motion of the winding machine model, and the winding machine model will feed back the interference information to the hardware control system at the same time. Thus, the motion information during the simulation is recorded through the SQL database which can help users to verify whether the control program logic is consistent with the conception.

1.3 Design of hardware control system

1.3.1 Hardware design

Mitsubishi (Japan) FX5U-PLC is used as the hardware controller, because the PLC-related control interface is simple, and has a high degree of integration and easy maintenance. While C# WinForm is used as the programming software for the user host.

The circuit board is the hub connecting PLC and the virtual simulation platform, whose main roles are: collecting the signals output (level signals, pulse signals, data signals transmitted through Modbus, etc.) from PLC and sending them to the virtual simulation platform; receiving the virtual sensor signals output from the virtual simulation platform and feedbacking to PLC.

According to the role of the circuit board, its overall architecture is designed as shown in Fig. 6.

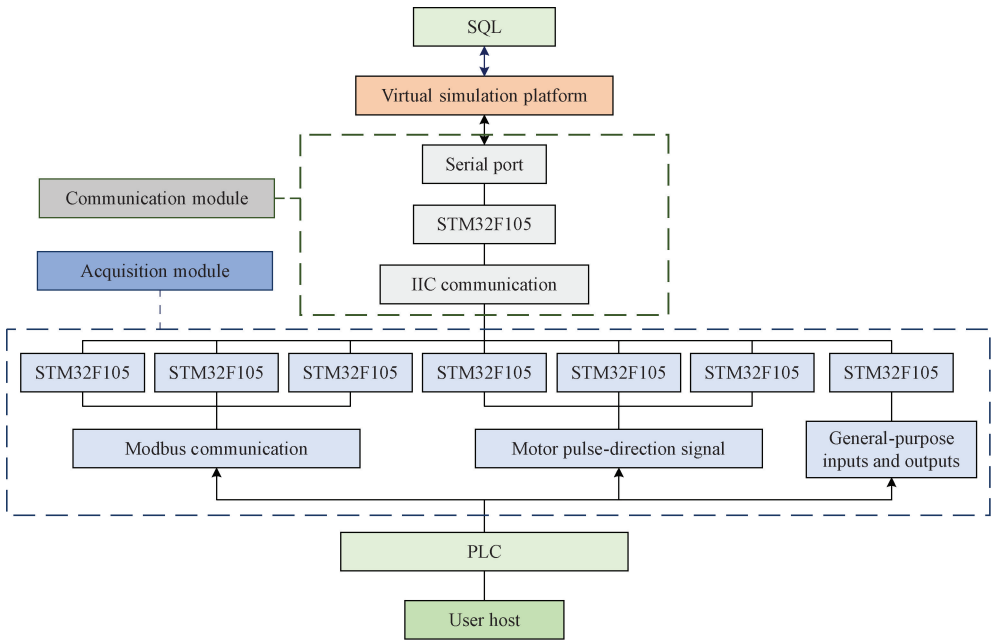

Fig. 6 Overall architecture of circuit board

The circuit board is mainly divided into the acquisition module and the communication module, and both modules use the STM32F105RBT6 chip based on the cortexM3 core.

1) Acquisition module. In order to simplify the procedure, one acquisition chip only acquires the signal of one motor, and the input and output (IO) signal of PLC is also acquired by a separate chip. During the operation of the winding machine, the output signals of PLC control a total of six motors. Among them, the two spindle axis motors and the contact roller motor are Modbus controllers, and the turntable motor and traverse motors are controlled by servos. Therefore, the acquisition module has seven STM32F105RBT6 acquisition chips, including three Modbus slaves, three motor pulse-direction signal acquisition and one general-purpose IO acquisition.

2) Communication module. The communication module also takes STM32F105RBT6 as the main control chip, the IIC communication is adopted between the main chip and each acquisition chip, and the communication between the main chip and the virtual simulation platform is through the serial port.

1.3.2 Software design

The data transmitted from the circuit board to the virtual simulation platform include Modbus frequency signals, pulse and direction signals and other switching input signals. The data received by the circuit board from the virtual simulation platform are servo motor origin signals, servo motor limit signals and virtual sensor signals. For these different signals, it is necessary to design the data storage and transmission methods.

The rotational speeds of the spindle and contact roller motors are sent from PLC to the circuit board, and in order to facilitate data transmission, the frequency data is sent directly to the circuit board. Thus, the frequency data of each motor is stored as a 16-bit variable. The pulse number of the traverse motor is converted to a rotational speed signal at the time of acquisition, and its data type is the float type, so it is stored in a 32-bit variable. For the contact roller and the turntable motor, the number of pulses is stored in a 32-bit variable due to the high frequency of pulse sending.

Because of the different data types, a structure is defined to store each motor and input signal. As shown in Table 1, when being sent to the virtual simulation platform, it needs to be unpacked and reloaded, that is, a corresponding size of the uint8_t type of array used to load the structure split out of the elements and sent sequentially through the serial port.

Table 1 Input data storage unit planning table

Data type and data name	Description	Byte
Short SSA	Motor frequency of spindle A	2
Short SSB	Motor frequency of spindle B	2
Short SC	Motor frequency of contact roller	2
Float ST	Traverse motor speed	4
Int PR	Number of pulses in turntable motor	4
Int PL	Number of pulses in lift motor	4
Uint8_t input	Solenoid valve input signal	1

The output signals include motor limit signal and cylinder limit signal, so two 8-bit variables are used to store the output signal data as shown in Table 2.

Table 2 Output data storage unit planning table

Data type	Description	Byte
Uint_8 limit	Motor limit signal	1
Uint_8 output	Cylinder limit signal	1

1.3.3 Winding control algorithm

The winding control algorithm used is the layered precision winding method. It is mainly based on the winding angle and the winding ratio (the number of revolutions of the spindle spools that the transverse wire guide reciprocates once), and is a more popular method. If the winding ratio is a positive integer, it is the stacking point of spinning. When the winding ratio is unchanged during the winding process, the winding angle will gradually increase as the diameter increases, but the winding angle has a minimum value limitation. If the winding angle is too small, it will lead to an increase in the number of yarns at the ends of the filament cake, which will lead to the phenomenon of convex edges. Therefore, when the winding angle is less than a certain value, it is necessary to recalculate the winding ratio. A fixed winding ratio is used within each layer, which varies from layer to layer, and precision winding is performed within each layer.

2 Winding Machine Working Principle

2.1 Workflow

The main structures of the winding machine system are the raw head, the winding device, the traverse device and the automatic change device. A typical winding machine structure is shown in Fig. 7.

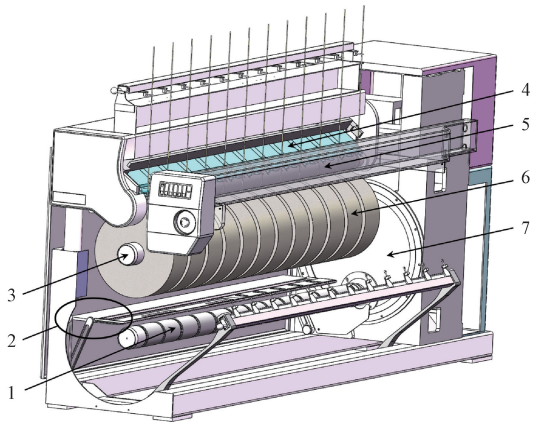

1— spindle B; 2— wire cutter; 3— spindle A;
4— traverse toggle; 5— contact roller; 6— package; 7— turntable.
Fig. 7 Main structure of winding machine

A complete winding cycle needs to go through five phases as shown in Fig. 8: a quick start phase, a top-speed holding phase, a winding phase, a deceleration phase and an unwinding phase. The raw head operation is generally carried out in the top-speed holding phase.

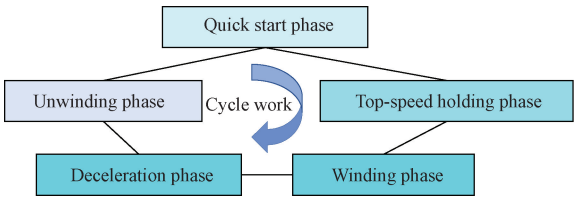

Fig. 8 A complete winding cycle

In order to ensure constant linear-speed winding, the spindle speed varies non-linearly during the winding phase. At the same time, the position change between the spindle and the contact roller in this phase is also more complicated. Therefore, this paper mainly focuses on the change of the spindle rotational speed and the position change between the spindle shaft and the contact roller in the winding phase.

2.2 Mathematical modeling

In the process of filament winding, the contact pressure between the contact roller and packages is an important factor affecting the forming of the winding. Nowadays, most winding machines use the triangle switching technology, that is, by slowly controlling the rotation of the turntable to regulate the contact pressure between the contact roller and packages. Figure 9 shows the schematic diagram of the contact between the contact roller and the packages.

In Fig. 9, β is defined as the contact pressure angle, indicating the angle between the vertical straight line through the center of the contact roll and the line joining the contact roll and the center of the package.

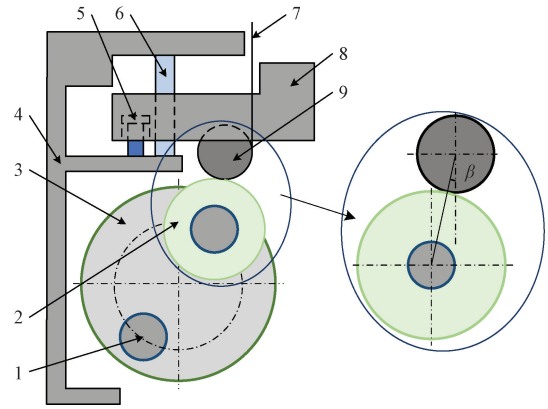

1—spindle B; 2—spindle A (packages); 3—turntable; 4—frame;
5—contact roller cylinder;6—smooth column; 7—yarn;
8—traverse box; 9—contact roller.
Fig. 9 Schematic diagram of contact between contact roller and packages

During the actual winding process, a displacement is generated when the diameter of packages increases and the turntable is rotated by a certain angle to counteract this displacement. This control principle is used in the simulation system and it is necessary to clarify the relative position change between the contact roller and packages. Therefore, the mathematical model is established among the contact roller, packages and the turntable.

2.2.1 Relative position change model of contact roller and packages

In the stage of the filament winding process, the relative position change between the contact roller and packages can be divided into four stages, as shown in Fig. 10. The symbols in Fig. 10 are described in Table 3.

1) After the paper tube on the spindle A is wound around the filament raw head, the turntable is immediately turned to the initial position, and the contact roller is in contact with the paper tube on the spindle A, as shown in Fig. 10(a).

2) As the diameter of the packages continues to increase until the thickness of the filament layer of the packages reaches about 20 mm[22], the normal contact pressure is applied, and the contact roller remains fixed relative to the frame thereafter, as shown in Fig. 10(b).

3) As the winding continues, the diameter of the packages continues to increase, and the turntable slowly rotates at a certain angle to maintain a constant contact pressure. When the center of the contact roller and the center of the packages are located in the same vertical straight line, the angle of the contact pressure is zero, as shown in Fig. 10(c).

4) Packages increase to full roll, and the turntable switches to the next winding cycle, as shown in Fig. 10(d).

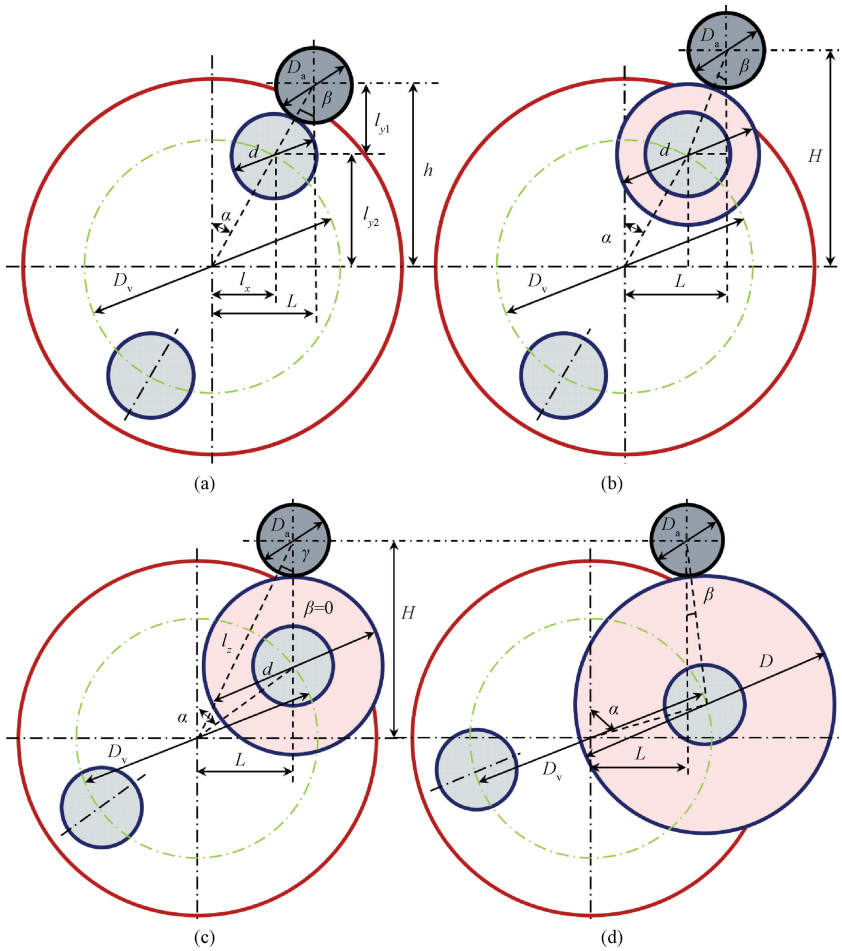

Fig. 10 Variation of relative positions between contact roller and packages: (a) initial winding; (b) $h_{max} = H$; (c) $\beta = 0$; (d) $d_{max} = D$

Table 3 Symbol description

Symbol	Description
D_a	Diameter of the contact roller (constant value)
D_v	Diameter of the virtual circle centered on the turntable center over the spindle center (constant value)
L	Horizontal distance between the contact roller center and the turntable center (constant value)
d	Diameter of the package
α	Angle of spindle axis A with respect to the turntable center
γ	Angle of the spindle center with respect to the line between the turntable center and the contact roller center
h	Vertical distance between the contact roller center and the turntable center
l_x	Horizontal distance between the spindle center and the turntable center
l_{y1}	Vertical distance between the contact roller center and the spindle center
l_{y2}	Vertical distance between the spindle center and the turntable center
l_z	Distance between the contact roller center and the turntable center

2.2.2 Mathematical model solution

According to the model of the relative position change between the contact roller and packages, the corresponding displacement of the cylinder of the contact roller Δh or the rotation angle of the turntable $\Delta\alpha$ can be found when the diameter of the packages increases.

Set the ith moment of winding as $\alpha = \alpha_i$ and $d = d_i$ ($i = 0, 1, \cdots, p, \cdots, q, \cdots, r$).

1) At winding moments in $0 \leqslant i \leqslant p$ (Figs. 10(a)–10(b)), the contact roller cylinder moves, the turntable does not move, and then

$$\begin{cases}\sin\beta_i=\dfrac{L-l_x}{(D_a+d_i)/2},\\ \sin\alpha_0=\dfrac{l_x}{D_v/2},\end{cases}\Rightarrow\begin{cases}\beta_i=\arcsin\left(\dfrac{2L-D_v\sin\alpha_0}{D_a+d_i}\right),\\ \alpha_i=\arcsin\left[\dfrac{2L-(D_a+d_i)\sin\beta_i}{D_v}\right],\end{cases}\tag{1}$$

$$\begin{cases}\cos\beta=\dfrac{l_{y1}}{(D_a+d)/2},\\ \cos\alpha_0=\dfrac{l_{y2}}{D_v/2},\end{cases}\Rightarrow h_i=l_{y1}+l_{y2}=\frac{(D_a+d_i)\cos\beta_i+D_v\cos\alpha_0}{2},$$

$$\Rightarrow\Delta h=h_{i+1}-h_i=\frac{1}{2}[(D_a+d_{i+1})\cos\beta_{i+1}-(D_a+d_i)\cos\beta_i],\tag{2}$$

$$\Delta\alpha=\alpha_{i+1}-\alpha_i=0.\tag{3}$$

2) At winding moments in $p<i\leqslant q$ (Figs. 10(b)–10(c)), the contact roller cylinder does not move, the turntable moves, and then

$$\begin{cases}\cos\gamma=\dfrac{[(D_a+d_i)/2]^2+l_z^2-(D_v/2)^2}{2\sqrt{L^2+H^2}[(D_a+d_i)/2]},\\ \tan(\gamma+\beta)=L/H,\end{cases}\Rightarrow\beta_i=\arctan\left(\frac{L}{H}\right)-\arccos\left[\frac{(D_a+d_i)^2+4L^2+4H^2-D_v^2}{4(D_a+d_i)\sqrt{L^2+H^2}}\right],\tag{4}$$

$$\Delta h=0,\tag{5}$$

$$\Delta\alpha=\arcsin\left[\frac{2L-(D_a+d_{i+1})\sin\beta_{i+1}}{D_v}\right]-\arcsin\left[\frac{2L-(D_a+d_i)\sin\beta_i}{D_v}\right].\tag{6}$$

3) At winding moments in $q<i\leqslant r$ (Figs. 10(c)–10(d)), the contact roller cylinder does not move, the turntable moves, and then

$$\begin{cases}\cos\gamma=\dfrac{[(D_a+d_i)/2]^2+l_z^2-(D_v/2)^2}{2\sqrt{L^2+H^2}[(D_a+d_i)/2]},\\ \tan(\gamma-\beta)=L/H,\end{cases}\Rightarrow\beta_i=\arccos\left[\frac{(D_a+d_i)^2+4L^2+4H^2-D_v^2}{4(D_a+d_i)\sqrt{L^2+H^2}}\right]-\arctan\left(\frac{L}{H}\right),\tag{7}$$

$$\Delta h=0,\tag{8}$$

$$\Delta\alpha=\arcsin\left[\frac{2L+(D_a+d_{i+1})\sin\beta_{i+1}}{D_v}\right]-\arcsin\left[\frac{2L+(D_a+d_i)\sin\beta_i}{D_v}\right].\tag{9}$$

2.2.3 Mathematical model implementation in Unity3D

The package diameter is changed according to the rotational speed of the spindle motor, and the scale of the package model along the z-axis direction is used to simulate the package diameter in Unity3D. A fixed step is set, and when the model scale changes and the scale difference reaches the fixed step, it is converted into the displacement of the contact roller cylinder and the angle of the turntable rotation according to Eqs. (1)–(9) in Subsection 2.2.2, as shown in Fig. 11. During the winding process, if there is a collision or interference, names, coordinates and time of the colliding object will be displayed on the window interface of Unity3D and recorded in SQL, as shown in Fig. 12.

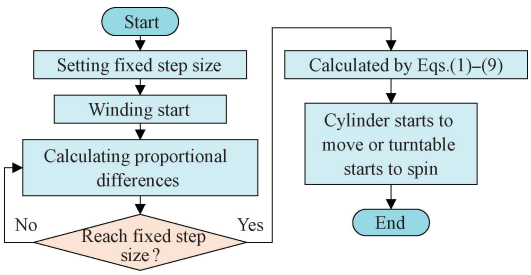

Fig. 11 Motion matching flowchart

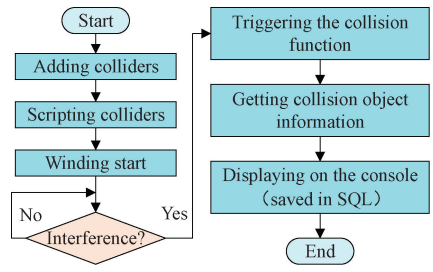

Fig. 12 Interference detection flowchart

3 Simulation System Verification

3.1 Simulation system construction

According to the overall scheme design of the simulation system, with the winding machine as the simulation object, the HILS system is constructed as shown in Fig. 13. In order to simplify the simulation of the control system, the main simulation is carried out on the motion coordination and the change of the spindle speed during the winding stage.

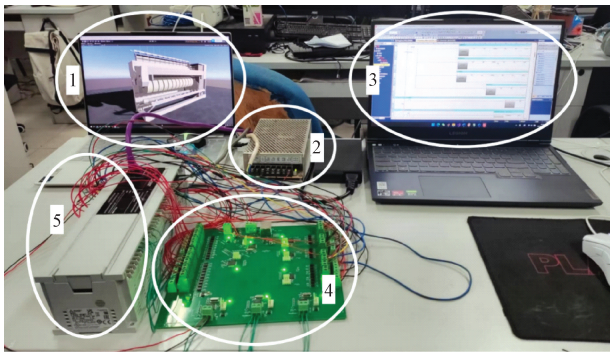

1— virtual simulation platform; 2— switching power supply; 3— user host; 4— simulation circuit board; 5— FX5U PLC.

Fig. 13 Physical connection diagram of HILS system

3.2 Real-time performance index of simulation system

In order to ensure the reliability of the simulation system, it is necessary to carry out the study of the real-time performance index. The real-time performance is mainly determined by the sampling frequency of external signals, the polling time of Modbus RTU communication, the frequency of IIC communication and serial port communication, and the number of refresh frames of the virtual simulation platform. Through the test of FX5U PLC, it can be seen that the highest acquisition pulse frequency of the simulation system can be up to 1 MHz, the Modbus RTU communication polling time is about 120 ms, the IIC communication and serial port communication frequency are 12 500 Hz and 115 200 bit/s, respectively, the number of refresh frames of the virtual simulation platform is 2 000 frame/s, and the variable-speed interval needs to be greater than 1 s. Thus the communication speed meets requirements.

3.3 Analysis of simulation results

The hardware control system controls the movement of the winding machine model in the virtual simulation platform through the real control procedure, and the movement beats and the position of the winding machine model are recorded in real time during the simulation process to generate the movement timing. After the simulation system runs, the spindle A/B speed, the contact roller speed, the transverse blade speed, the contact roller cylinder displacement, and the turntable rotation angle are shown in Fig. 14.

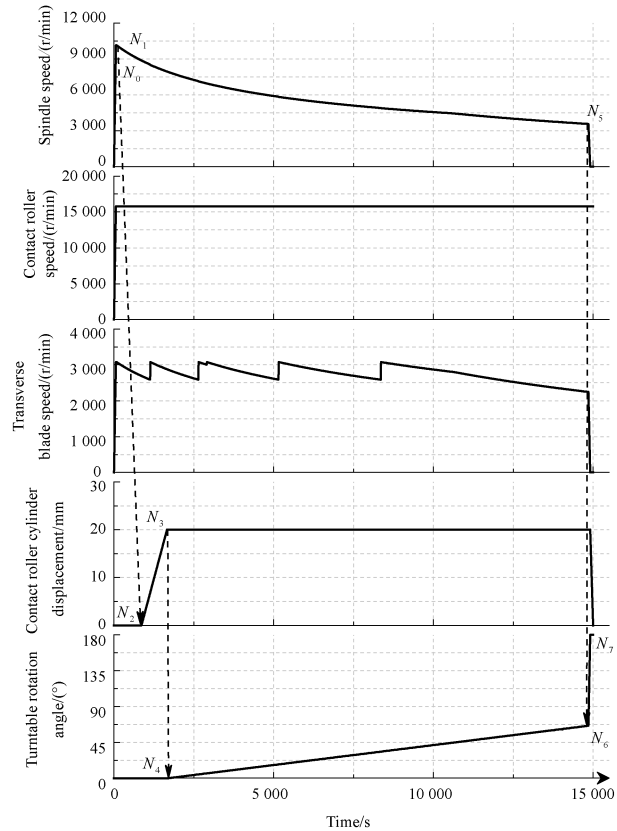

Fig. 14 Timing diagram of motion of a complete winding cycle

At first, the contact roller, the traverse blade and the spindle A start quickly, and the spindle A is accelerated to the N_0 position and holds for a period of time to the N_1 position for raw-head operation. Then the contact roller cylinder is prepared for action and is raised as the thickness of the filament layer of the package increases, from the N_2 position to the N_3 position. The N_3 position indicates that the contact roller cylinder has risen to the maximum height and is held fixed, and that the contact roller can apply the normal pressure to the package. Thereafter, the contact pressure is maintained constant by rotating the turntable, which rotates from the N_4 position to the N_6 position; when the spindle speed decreases nonlinearly to the N_5 position, the full package is reached, and the turntable rotates considerably, from the N_6 position to the N_7 position. At this time, the drop phase begins, the spindle B switches to the upper, the cutter on the back plate carries out the action, and finally waiting for the spindle A to stop rotating, the pusher cylinder unloads the full package from the spindle A, and it is carried by the handling robot to the shelving area.

In Subsection 2.2.2, the changes among contact rollers, packages and turntables during the winding stage are analyzed, and the function scripts are mounted on the corresponding objects. Figure 15 shows the 3D effect of contact rollers, packages and turntables in Unity3D during the winding stage in the simulation run.

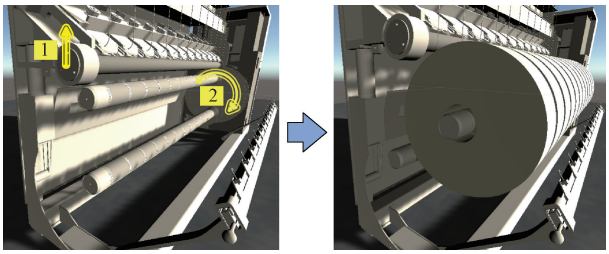

1—winding moment in $0 \leqslant i \leqslant p$; 2—winding moment in $p < i \leqslant q$.
Fig. 15 Changes during winding stage

By observing and analyzing the motion timing output from the simulation system, it can be verified that the system control program is written without error and conforms to the workflow.

4 Conclusions

This paper develops and designs a set of the HILS system with the winding machine as the simulation object, which can simultaneously meet the requirements of a better 3D display effect, and a real-time and connecting mechatronic software for comprehensive simulation. After the simulation operation, the main conclusions are obtained.

1) By observing the movement of the winding machine in Unity3D, it is verified that the system has a good real-time and 3D display effect.

2) The functionality and the effectiveness of the system are verified by analyzing the timing of key actions during the operation of the winding machine.

In summary, the application of semi-physical simulation technology in the winding machine allows developers to complete the debugging of the control program in the laboratory, which is of great significance for the subsequent debugging of other textile machinery research and development, optimization of program logic, system design and process development.

References

[1] LEDIN J A. Hardware-in-the-loop simulation [J]. *Embedded Systems Programming*, 1999, 12: 42-62.

[2] ISERMANN R, SCHA J. Hardware-in-the-loop simulation for the design and testing of engine-control systems [J]. *Control Engineering Practice*, 1999, 7(5): 643-653.

[3] CHUNG Y, YANG Y P. Hardware-in-the-loop simulation of self-driving electric vehicles by dynamic path planning and model predictive control[J]. *Electronics*, 2021, 10(19): 2447.

[4] SAHOO S R, CHIDDARWAR S S. Flatness-based control scheme for hardware-in-the-loop simulations of omnidirectional mobile robot[J]. *Simulation*, 2020, 96(2): 169-183.

[5] OMAR H M. Hardware-In-the-loop simulation of time-delayed anti-swing controller for quadrotor with suspended load [J]. *Applied Sciences*, 2022, 12(3): 1706.

[6] KIM N, KIM H, LEE W. Hardware-in-the-loop simulation for estimation of position control performance of machine tool feed drive [J]. *Precision Engineering*, 2019, 60: 587-593.

[7] BASLER M, LEISTEN C, JASSMANN U, et al. Experimental validation of inertia-eigenfrequency emulation for wind turbines on system test benches[C]//IECON 2020 the 46th Annual Conference of the IEEE Industrial Electronics Society. New York: ACM, 2020: 205-212.

[8] MORETTI G, SCIALÒ A, MALARA G, et al. Hardware-in-the-loop simulation of wave energy converters based on dielectric elastomer generators[J]. *Meccanica*, 2021, 56(5): 1223-1237.

[9] SALEHI A, MONTAZERI-GH M. Hardware-in-the-loop simulation of fuel control actuator of a turboshaft gas turbine engine[J]. *Proceedings of the Institution of Mechanical Engineers, Part M: Journal of Engineering for the Maritime Environment*, 2019, 233(3): 969-977.

[10] RESCH S, FRIEDRICH J, WAGNER T, et al. Stability analysis of power hardware-in-the-loop simulations for grid applications[J]. *Electronics*, 2021, 11(1): 7.

[11] KOTSAMPOPOULOS P, LAGOS D, HATZIARGYRIOU N, et al. A benchmark system for hardware-in-the-loop testing of distributed energy resources[J]. *IEEE Power and Energy Technology Systems Journal*, 2018, 5(3): 94-103.

[12] ZHANG X, XIE X R, SHAIR J, et al. A grid-side subsynchronous damping controller to mitigate unstable SSCI and its hardware-in-the-loop tests[J]. *IEEE Transactions on Sustainable Energy*, 2020, 11(3): 1548-1558.

[13] ABRAZEH S, MOHSENI S, ZEITOUNI M J, et al. Virtual hardware-in-the-loop FMU co-simulation based digital twins for heating, ventilation, and air-conditioning (HVAC) systems [J]. *IEEE Transactions on Emerging Topics in Computational Intelligence*, 2022, 7(1): 65-75.

[14] SHIN S Y, CHAOUCH K, NEJATI S, et al. Uncertainty-aware specification and analysis for hardware-in-the-loop testing of cyber-physical systems[J]. *Journal of Systems and Software*, 2021, 171: 110813.

[15] XIE B, WANG S, WU X H, et al. Design and hardware-in-the-loop test of a coupled drive system for electric tractor [J]. *Biosystems Engineering*, 2022, 216: 165-185.

[16] LIU P F, ZHENG M Y, NING D H, et al. Decoupling vibration control of a semi-active electrically interconnected suspension based on mechanical hardware-in-the-loop[J]. *Mechanical Systems and Signal Processing*, 2022, 166: 108455.
[17] KARPENKO M, SEPEHRI N. Hardware-in-the-loop simulator for research on fault tolerant control of electrohydraulic actuators in a flight control application[J]. *Mechatronics*, 2009, 19(7): 1067-1077.
[18] AMER N H, HUDHA K, ZAMZURI H, et al. Hardware-in-the-loop simulation of trajectory following control for a light armoured vehicle optimised with particle swarm optimisation[J]. *International Journal of Heavy Vehicle Systems*, 2019, 26(5): 663.
[19] YU Z Q, ZHANG Y M, JIANG B, et al. Nussbaum-based finite-time fractional-order backstepping fault-tolerant flight control of fixed-wing UAV against input saturation with hardware-in-the-loop validation[J]. *Mechanical Systems and Signal Processing*, 2021, 153: 107406.
[20] KHOOBAN M H. Hardware-in-the-loop simulation for the analyzing of smart speed control in highly nonlinear hybrid electric vehicle[J]. *Transactions of the Institute of Measurement and Control*, 2019, 41(2): 458-467.
[21] WU H, ZOU K, TANG L, et al. Semi-physical simulation system of robots for lawn carpet repair based on Unity3D[J]. *Journal of Donghua University (Natural Science)*, 2024, 50(1): 85-92. (in Chinese)
[22] WANG Y X, ZHANG L J, HOU X, et al. A dynamic modeling approach for the winding spindle during start-up with a coupled flexible support system[J]. *Textile Research Journal*, 2020, 90(7/8): 757-775.

基于 Unity3D 的卷绕机半物理仿真系统研究

唐 龙，邹 鲲*
东华大学 机械工程学院，上海 201620

摘 要：机电一体化产品在研发过程中普遍面临现场调试工作量大、周期长和成本高等问题，而且目前主流的仿真软件功能较为单一。因此，研究设计了一套兼具实时性和三维展示效果、能够连接机械电子软件的半物理仿真系统。其以卷绕机为仿真对象，利用 Unity3D 搭建虚拟仿真平台，通过电路板实现虚拟仿真平台与控制系统间数据的实时交互。通过输出卷绕过程中关键结构的运动时序和空间轨迹图，验证了卷绕机机电系统的工艺仿真可行性。研究结果表明，该系统可替代部分现场调试工作，提高研发效率。

关键词：半物理仿真；卷绕机；实时性；Unity3D；三维展示；仿真电路板；工艺仿真